EXPERIMENTAL MEASUREMENTS OF SPREADING OF VOLATILE LIQUID DROPLETS

Nengli Zhang*, David F. Chao†

*Ohio Aerospace Institute at NASA Glenn Research Center, Cleveland, OH 44135, USA, †NASA Glenn Research Center, Cleveland, OH 44135, USA

ABSTRACT

Based on the laser shadowgraphic system used by the first author of the present paper, a simple optical system, which combined the laser shadowgraphy and the direct magnified-photography, has been developed to measure the contact angle, the spreading speed, and the evaporation rate. Additionally, the system can also visualize inside thermocapillary convection of a sessile drop simultaneously.

The experimental results show that evaporation/condensation and thermocapillary convection in the sessile drop induced by the evaporation strongly affects the wetting and spreading of the drop. Condensation always promotes the wetting and spreading of the drop. Evaporation may increase or decrease the contact angle of the evaporating sessile drops, depending on the evaporation rate. The thermocapillary convection in the drop induced by the evaporation enhances the effects of evaporation to suppress the spreading.

INTRODUCTION

The spreading of an evaporating liquid on a solid surface occurs in many practical processes, including thermal engineering. The typical processes concerned with heat transfer are film cooling, heat transfer in boiling and heat pipes.

Spreading of nonvolatile liquid droplets on a horizontal solid surface is a simple and useful tool in the study of the free-boundary problem, and therefore has been well studied by many investigators. A comprehensive review was made by Leger and Joanny [1]. The lack of volatility of the liquid implies the conservation of mass and volume, and thus simplifies the theoretical analysis. However, the occurrence of evaporation of common liquids is inevitable in practical processes. A well understanding of the evaporation influences on the contact angle of the droplet in controlled environment conditions is important in the study of the spreading. Recently, Anderson and Davis [2] analytically studied spreading of a two-dimensional volatile liquid droplet on a uniformly heated horizontal surface using lubrication theory. Hocking [3] considered that the macroscopic contact angles deviates from the microscopic angle in slip region and found that the contact angle is increased by evaporation. Moosman and Homsy [4] also reported an increase in the apparent contact angle when evaporation is present. However, Shanahan and Bourgès [5, 6] concluded that evaporation from the liquid drop meniscus will lower the contact angle. Anderson and Davis also found the effects of Marangoni flow induced by the local surface tension gradient near the contact line on the spreading through their analysis. However, the Marangoni flow direction found in their study is directly opposite from that observed in Cazabat et al. [7] and Redon et al. [8]. Obviously, these contradictions indicate that the dominant mechanism of the spreading of the evaporating drop is not clear yet. Further experimental studies using appropriate techniques are needed.

The most common method to measure the contact angle, the contact radius, and the height of a sessile drop on a solid surface is to view the drop from its edge through an optical microscope. This method can give only local information in the view direction. Zhang and Yang [9, 10] developed a laser shadowgraphy method to investigate the evaporation of sessile drop on a glass plate. The whole periphery of the drop can be tested simultaneously and the instantaneous drop size, including the contact diameter, the maximum height of the drop, and volume-time history can be determined. Allain et al. [11] used the same method to measure the contact angle of sessile drops. Due to the fuzzy outer rim of the projected shadow of the drop for the diameter of the drop is only an order of 1 mm, a considerable large error resulted in the measurement. This problem becomes more serious for a volatile liquid sessile drop when its base diameter contracts rapidly during the evaporation. Based on the laser shadowgraphy method developed by Zhang and Yang, we suggested a new optical arrangement to measure the contact angle and the evaporation rate of a sessile drop with much higher accuracy [12, 13].

The present study focuses attention on the effects of evaporation/condensation and thermocapillary convection on the spreading process and the evolution of the contact angle.

EXPERIMENTAL METHOD

A hybrid optical system of laser shadowgraphy and direct photography developed by Zhang and Chao [12, 13] was used in the present study. The hybrid optical system is briefly schematically shown in Fig. 1. A laser beam and a white light beam were collimated to horizontally parallel beams and then reflected by a splitter to perpendicularly pass through a test section without obstructing to view the tested drop from top. The test section was made of a microscope glass slide as the bottom and four pieces of plastic plate as the side walls. Two liquid reservoirs were put in the test section. For the experiment of the drop spreading in the saturated vapor environment, using another 1 mm thick rectangular microscope glass slide to cover the test section, sealed with Dow Corning high vacuum grease to form a hermetic box. The two glass slides were adjusted to parallel each other enabling the parallel lights passing through the drop vertically and the drop being viewed from top without distortion. In order to create a nonsaturated vapor environment three pieces of 1 mm thick microscope glass slides were used to constitute the cover. One was used as the main cover and fixed at the middle of the test section with the vacuum grease, which was adjusted to parallel with the bottom of the test section. Others were placed at the both sides of the main cover and can be slid laterally to function as a shutter to control the opening of the cover. It should be noted that the evaporation/condensation rate of the sessile drop varies with the vapor environment and dramatically affects the spreading characteristics of the drop. Therefore, we measured the evaporation/condensation rate through the volume-time history of the tested drop rather than the saturation level.

The laser beam was used to produce a refractive image of the sessile drop on a screen and white beam was used to get shaper photograph of the top view of the drop. The refractive image on the screen was recorded by a video recording system (system I), which constituted by a CCD camera with a video recorder and a monitor. Meanwhile, another video recording system (system II) was used to record the top view of the sessile drop. Both the recording systems can replay frame-by-frame with 30 frames per second.

Before each test the bottom glass slide of the test section was cleaned by ethanol and wiped by Olympus lens cleaning tissues, and then was shelved in open air, covered by a soft tissue, at least 24 hours. The bottom slide surface then became free of residual liquid molecules while remaining intact from impurity of the ambient air. The tested liquid was carefully deposited on the bottom surface by a micro-syringe to form a 1.5 to 4 μl sessile drop. The origin of the spreading and evaporation time, t, was taken at the moment when the micro syringe was detached from the liquid body.

The evolution of contact diameter, $d(t)$, is directly measured by the top view recorded by the recording system I. The tested drops are relatively small and are not deformed significantly by gravitational effects and therefore, can be considered to be sphere caps functioning as a plano-convex lens with a good approximation. The method developed by Zhang and Yang [9] is used to determine the evolution of the contact angle, $\theta(t)$, and the volume of the drop, $V(t)$. By a vary simple geometric relationship, the following expressions were derived:

$$\theta(t) = Arc\sin\frac{d(t)}{2\cdot R(t)} \tag{1}$$

$$V(t) = \pi\cdot h^2(t)\cdot[R(t) - \frac{h(t)}{3}] \tag{2}$$

Here, $h(t)$ is the maximum instant height of the sphere cap which is determined by

$$h(t) = R(t) - \sqrt{R^2(t) - d^2(t)/4} \tag{3}$$

where $R(t)$ is the instant curvature radius of the liquid sphere cap, which can be calculated from $R(t) = (n-1)\cdot s\cdot d(t)/[D(t)+d(t)]$, where n is the refractive

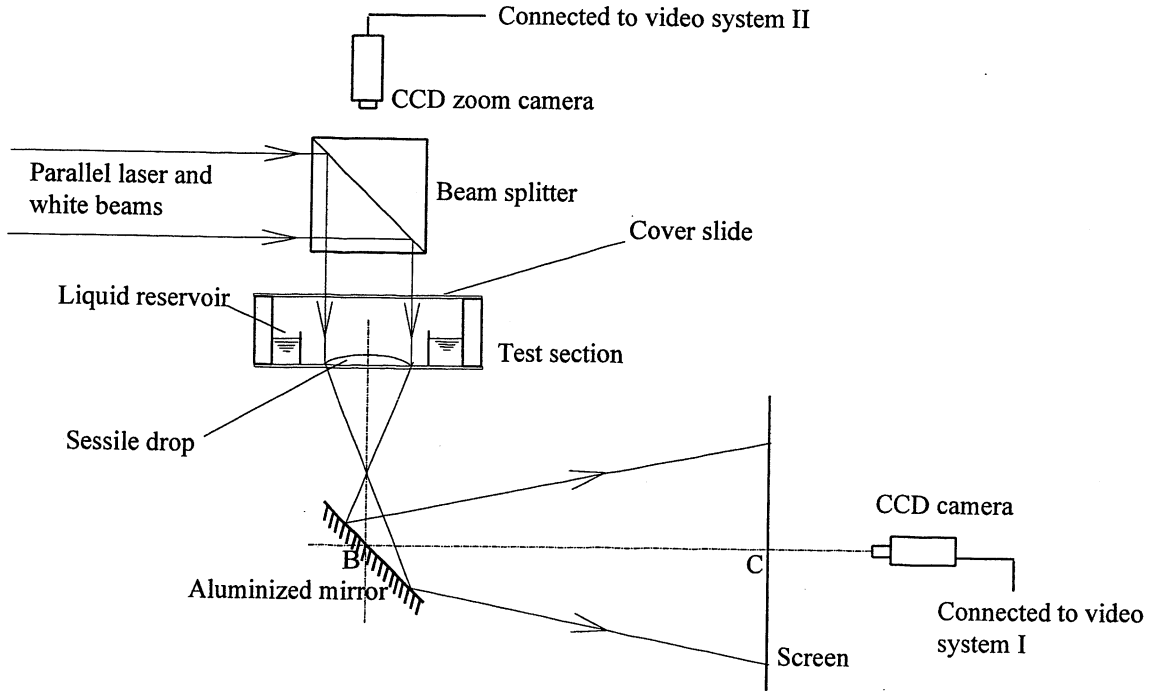

Fig. 1 Hybrid optical arrangement for measurements of spreading and contact angle

index of the liquid, s is the drop-screen distance from the center considered as an important parameter to measure the evaporation strength which can be determined by

$$\overline{w} = \frac{V_o}{t_f} \tag{4}$$

where V_o is the initial volume of the sessile drop (the drop volume at $t=0$), t_f is the lifetime of the tested drop. The instant evaporation rate, $W(t)$, can be calculated by $W(t)=\Delta V(t)/\Delta t$, where $\Delta V(t)$ is the difference of volumes between the measuring time interval Δt.

Figure 2 shows a typical picture of the drop top view and its correspondent refractive image on the screen with the drop-screen distance, s, of 630.0 mm. The pictures were taken at the moment of 1.97 sec. after an R-113 drop of 4 μl was placed on the bottom surface of the test section in open air at the room temperature 24 °C and the relative humidity of 44%. It can be seen that, from Fig. 2(a), $d(1.97)$=5.23 mm, and from Fig.2(b), $D(1.97)$=93.33 mm. Then, the instant contact angle, the maximum instant height of the drop, and the instant volume of the drop can be calculated from Eqs. (1) to (3): $\theta(1.97)$=12.704°, $h(1.97)$=0.291 mm, $V(1.97)$=3.140 mm^3.

RESULTS AND DISCUSSION

Three typical volatile liquids, freon-113 (R-113), cyclohexane, and n-pentane, were tested in different environments. The initial volume of the sessile drops was controlled less than 4 μl and therefore the drop profiles can be taken as sphere caps. Experimental results show that evaporation/condensation and Marangoni convection induced by the evaporation strongly affect the spreading. Condensation promotes the spreading, but evaporation suppresses the spreading and tends to advance a contraction of the drop. The competition between the spreading power and a weaker evaporation results in a complex spreading process with a change of the evolution trend of contact angle and contact diameter. Strong evaporation can hold back the spreading and pushes the drop to monotonically contract. Although the average evaporation rates between the tested liquids differ by one order of magnitude, all of them show that a capillary spreading process dominates in the initial stage and is gradually overtaken by the effects of evaporation.

Effects of Evaporation/condensation:

When an R-113 drop of 2.45 μl is placed on the glass surface in the saturated vapor environment at room temperature 24 °C, it rapidly spreads over on the surface. Due to the tendency of complete wetting, the contact diameter of the drop continuously increases and the drop finally becomes a thin film. The thickness of the wetting film results from a competition between long-range forces and spreading power, which is defined as

$$S = \gamma_{sv} - \gamma_{sl} - \gamma_{lv} \tag{5}$$

where γ_{sv} is the surface energy of interface between the solid and the vapor, γ_{sl} and γ_{lv} are the interface tension between the solid and the liquid, and the interface tension between the liquid and the vapor, respectively. As pointed out by Brochard-Wyart et al. [14], the long-range van der Waals forces tends to thicken the film, and the spreading power favors a large wet region. The major spreading process takes place within 1.5 seconds. Figure 3 (a) shows the evolution of the contact diameter, the contact angle, and the volume of the drop. Both the contact diameter and the volume of the drop monotonously increase while the contact angle decreases. The condensation at the contact line region plays a crucial role to renormalize the effective value of the spreading power making the drop completely wetting. The solid surface placed in the saturated vapor environment is certainly moistened, and therefore the physical chemistry properties of the surface are changed, especially the surface energy of the solid surface. It serves the mechanism of the variety of wetting characteristics.

The most complex and interesting case of this study is the drop spreading under a nonsaturated vapor environment. We tested a drop of 1.75 μl under the nonsaturated vapor environment at room temperature 24 °C, with an average evaporation rate of 0.032 μl/sec. The evolution of the contact

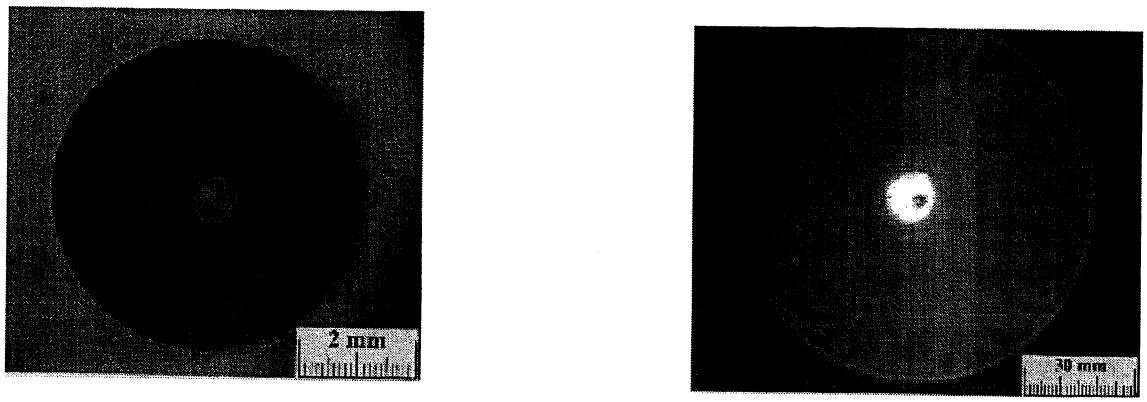

(a) Direct top view (b) Refractive image

Fig. 2 Typical picture of the top view of a sessile drop and its refractive image

diameter, the contact angle, and the drop volume is shown in Fig.3 (b). The whole process can be divided to three stages: 1) The drop rapidly spreads out on the surface first, promoted by condensation of the vapor. It is referred as condensation-spreading stage. In this stage, both the contact diameter and the drop volume increase while the contact angle decreases sharply. 2) When the evaporation dominants the mass transfer between the drop and the vapor environment, both the contact diameter and the drop volume decrease while the contact angle increases, referred as evaporation-retracting stage. In this stage, the competition between evaporation effects and the spreading power turns the spreading of the drop onto a continuous retraction. In the mean time, the contact angle remains at a constant value for a while and then successively increases. 3) When the drop contact diameter retracts to a certain value (here it is 2 mm), the contact angle turns to decrease and the drop contracts more and more rapidly till drying up, referred as rapid contracting stage. In this last stage, the decrease of both the contact diameter and the contact angle is gradually accelerated, though the evaporation rate is slowing down, due to the restrain of geometry relation.

Effects of Evaporation Rate:

In order to test the effects of evaporation rate on the drop spreading and the evolution of the contact angle, three volatile liquids, cyclohexane, n-pentane, and R-113, were tested in open-air environment at room temperature (23 °C) and relative humidity of 44%. Generally, four stages have been observed: (1) initial spreading; (2) spreading-evaporation competitive balance; (3) evaporation dominating contraction; and (4) final rapid contraction. The higher the evaporation rate is, the shorter the initial spreading exists. Typical cases are described as follows. A cyclohexane sessile drop of initial volume 1.91 μl has a lifetime 56.83 seconds with the average evaporation rate of 0.034 μl/sec. The drop rapidly spreads initially, expanding its contact diameter from 3.81mm to 5.01 mm within 3 seconds, and then maintains its contact diameter unchanged for about 1.5 seconds in which the effects of evaporation and spreading reach a competition balance. After evaporation dominates the evolution process the drop almost linearly contracts to about 2 mm in contact diameter and then rapidly contracts till vanishing, as shown in Fig. 4 (a). Correspondingly, an n-pentane sessile drop has much higher evaporation rate and so shorter spreading period. For example, an n-pentane drop of initial volume of 1.61 μl has a lifetime 7.2 seconds with the average evaporation rate of 0.22 μl/sec. The n-pentane drop has the same evolution behavior of the contact diameter as the cyclohexane drop, but spreads only 0.4 seconds, as shown in Fig. 4 (b). It is noted that the final rapid contraction stage also starts at the contact diameter of about 2 mm.

The evolution of contact angle of a sessile drop for different liquids is quite different. For drops with lower evaporation rates, the contact angle decreases in the initial spreading and the spreading-evaporation balance stages. It increases linearly in the evaporation-dominant contraction stage and then rapidly grows in the final rapid-contraction stage, as shown in Fig. 4 (a). Obviously, evaporation increases the contact angle because of a large evaporative loss near the drop edge. For the drops with higher evaporation rates, the contact angle decreases monotonically and has a contact-angle plateau in the evaporation-dominant contraction stage. Although the evaporation generally would increase the contact angle, at the point where the stronger evaporation consumes the liquid volume of the drop large enough the contact angle turns to decrease. The characteristics of the evolution of the contact diameter and the contact angle are shown in Fig. 4 (b) and (c).

It is of interest to note that although the evaporation rate of R-113 sessile drops is lower than that of n-pentane sessile drops, the initial spreading stage of an R-113 drop is much shorter than that of an n-pentane drop. For example, an R-113 sessile drop with an initial volume of 2.36 μl has a lifetime of 19.2 second, but the period of initial spreading stage has only 0.2 seconds, as shown in Fig. 4 (c). It is also noted that the spreading-evaporation balance stage is too short to detect. This implies that there is another physical process that affects the evolution of the contact diameter.

Effects of Thermocapillary Convection

Thermocapillary convection in sessile drops can be induced by evaporation only under certain conditions, depending on the properties of the volatile liquids. Of the three liquids tested in this study, the cyclohexane drops, with initial volumes of 1.5 μl to 5 μl, exhibit no convection throughout their lifetime. The convection in n-pentane drops occurs near the end of the second stage (the spreading-evaporation balance stage). For example, for the n-pentane drop with an initial volume of 1.61 μl, convection appears at about 1 second after the drop begins to spread. Before then there is no convection in the drop at all. However, the thermocapillary convection in the R-113 sessile drops is induced by evaporation from the very beginning, even before the syringe detaches from the drops. The typical image of the convection in the R-113 drops is shown in Fig. 2 (b).

Due to the strong thermocapillary convection in the R-113 sessile drops, the evolution of the contact diameter is different from that of both cyclohexane and n-pentane drops. The thermocapillary convection in sessile drops obviously prevents the drops from spreading, enhancing the evaporation effects to suppress the spreading in the evolution of contact diameter. That is why the R-113 drop has very short initial spreading stage comparing to n-pentane drop and an undetectable spreading-evaporation balance stage, though its evaporation rate is much lower than one of n-pentane. It is interesting to note that the R-113 drop accelerates contraction after its contact diameter reaches 2 mm, too.

Uncertainty analysis

The method of single sample experiments was utilized to estimate the uncertainties in both θ and V through Eqs. (1) and (2). The maximum uncertainty occurs in the end of the final stage for R-113 sessile drop evaporating in open air, in which d=0.82±0.019mm and D=76.2±0.22mm. The uncertainty for the contact angle is 2.78% and for the drop volume is 10.68%, respectively.

CONCLUSIONS

Experimental results of evaporating sessile drops on a glass-slide surface for three volatile liquids show that the evaporation/condensation and thermocapillary convection strongly affect the drop spreading and contact angle. The main conclusions are summarized as follows:

1. Evaporation/condensation plays a crucial role in the wetting and spreading of volatile liquid drops and greatly affects the evolution of the contact angle and the contact

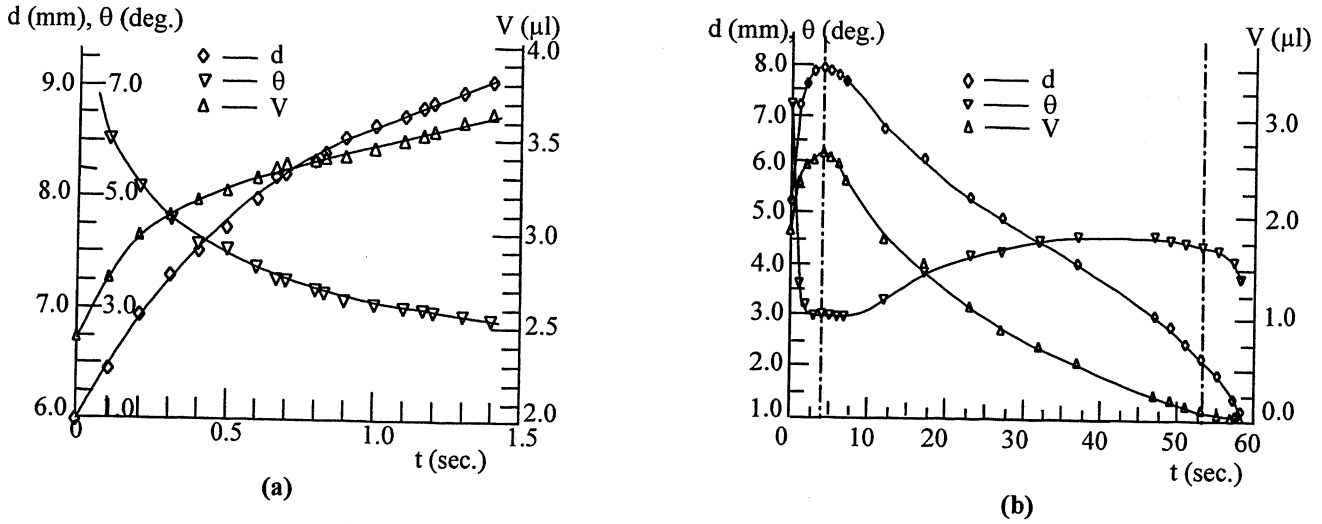

Fig. 3 Evolution of contact diameter, contact angle, and volume of an R-113 sessile drop: (a) in saturated vapor environment with initial volume of 2.45 μl, (b) in a nonsaturated vapor environment with initial volume of 1.75 μl.

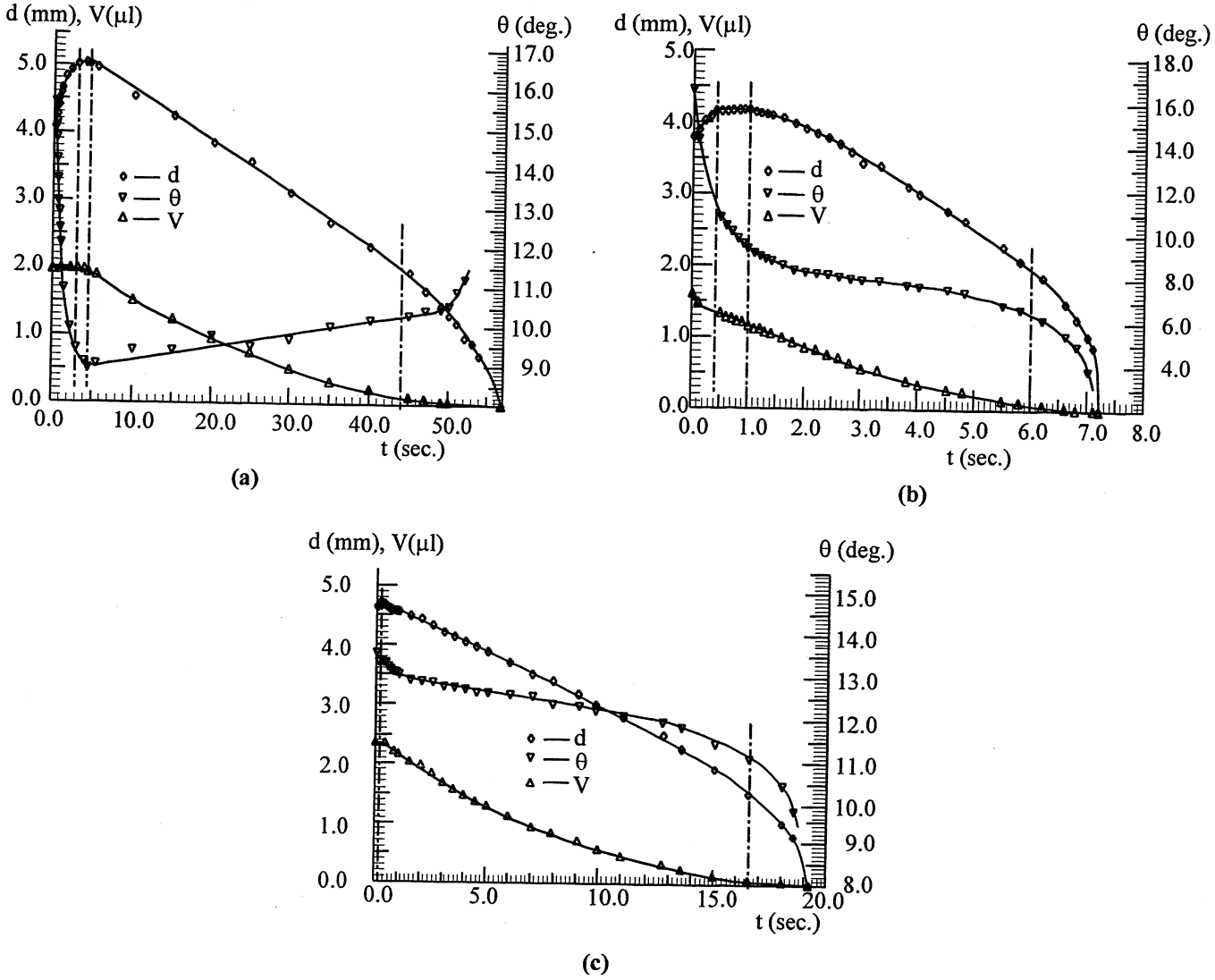

Fig. 4 Evolution of contact diameter, contact angle, and volume of a sessile drop in open air: (a) cyclohexane drop, (b) n-pentane drop, (c) R-113 drop

diameter of the drop. An R-113 drop placed in three different vapor environments presents quite different spreading characteristics. Condensation promotes the spreading, but evaporation suppresses the spreading and favors contraction of the drop. The competition between a weaker evaporation effects and the spreading power results in a complex spreading process turning the drop spreading onto a continuous retraction. Strong evaporation can hold back the spreading and pushes the drop to monotonically contract. When the contact diameter of an evaporating sessile liquid drop decreases to a certain value, the contraction of the drop is gradually accelerated till trying up, though the evaporation rate of the drop is slowing down.

2. An evolution of contact diameter of a sessile drop evaporating in open air can be divided into four stages: 1) initial spreading; 2) spreading-evaporation balance; 3) evaporation-dominant contraction; and 4) rapid contraction. Drop spreading always exists at the early initial spreading stage in the evolution of contact diameter of an evaporating liquid sessile drop, even if the drop has a considerably high evaporation rate, but is rapidly taken over by the effects of evaporation.
3. Thermocapillary convection induced by the evaporation enhances the evaporation effects on the evolution of the drop contact diameter and the contact angle to surpass the spreading and shortens the spreading-evaporation balance stage to become undetectable.
4. The contact angle of sessile drops with low evaporation rate is increased by evaporation. However, strong evaporation decreases the contact angle to create a contact-angle plateau in the evaporation-dominant contraction stage.
5. The evaporation of sessile drops always accelerates contraction when their contact diameter reaches 2 mm.

REFERENCES

1. L. Leger and J. F. Joanny, Liquid spreading, *Rep. Prog. Phys.*, pp. 431-486, 1992.
2. D. M. Anderson and S. H. Davis, The spreading of volatile liquid droplets on heated surfaces, *Phys. Fluids,* vol. 7, pp. 248-265, 1995.
3. L. M. Hocking, On contact angle in evaporating liquids, *Phys. Fluids,* vol. 7, pp. 2950-2955, 1995.
4. S. Moosman and G. M. Homsy, Evaporating menisci of wetting fluids, *J. Colloid Interface Sci.,* vol. 73, pp. 212-223, 1980.
5. M. E. R. Shanahan and C. Bourgès, Effects of evaporation on contact angles on polymer surfaces, *Int. J. Adhesion and Adhesives,* vol. 14, pp. 201-205, 1994.
6. C. Bourgès-Monnier and M. E. R. Shanahan, Influence of evaporation on contact angle, *Langmuir,* vol. 11, pp. 2820-2829, 1995.
7. A. M. Cazabat, F. Heslot, S. M. Troian, and P. Carles, Fingering instability of thin spreading films driven by temperature gradients, *Nature,* vol. 346, pp. 824-826, 1990.
8. C. Redon, F. Brochard-Wyart, and F. Rondelez, Festoon instabilities of slightly volatile liquids during spreading, *J. Phys. II (France),* vol. 2, pp. 1671-1676, 1992.
9. N. Zhang and W. J. Yang, Natural convection in evaporating minute drops, *J. Heat Transfer,* vol. 104, pp. 656-662, 1982.
10. N. Zhang and W. J. Yang, Visualization of evaporative convection in minute drops by laser shadowgraphy, *Rev. Sci. Instrum.,* vol. 54, pp. 93-96, 1983.
11. C. Allain, D. Ausserre, and F. Rondelez, A new method for contact-angle measurements of sessile drops, *J. Colloid Interface Sci.,* vol. 107, pp. 5-13, 1985.
12. N. Zhang and D. F. Chao, A new approach to measure contact angle and evaporation rate with flow visualization in a sessile drop, *International Conference on Interface Problems,* Aug. 16-18, 1999, Monterey, California, U.S.A. *and NASA/TM-1999-209636,* 1999.
13. N. Zhang, and D. F. Chao, Effects of Evaporation/Condensation on Spreading and Contact Angle of a Volatile Liquid Drop, *Heat Transfer Science and Technology 2000,* Higher Education Press, Beijing, pp. 367-372, 2000.
14. F. Brochard-Wyart, J. M. di Meglio, D. Quere, and P. G. Gennes, Spreading of nonvolatile liquids in a continuum picture, *Langmuir,* vol. 7, pp. 335-338, 1991.

EXPERIMENTAL MEASUREMENTS OF SPREADING OF VOLATILE LIQUID DROPLETS

Nengli Zhang*, David F. Chao†

*Ohio Aerospace Institute at NASA Glenn Research Center, Cleveland, OH 44135, USA, †NASA Glenn Research Center, Cleveland, OH 44135, USA

ABSTRACT

Based on the laser shadowgraphic system used by the first author of the present paper, a simple optical system, which combined the laser shadowgraphy and the direct magnified-photography, has been developed to measure the contact angle, the spreading speed, and the evaporation rate. Additionally, the system can also visualize inside thermocapillary convection of a sessile drop simultaneously.

The experimental results show that evaporation/condensation and thermocapillary convection in the sessile drop induced by the evaporation strongly affects the wetting and spreading of the drop. Condensation always promotes the wetting and spreading of the drop. Evaporation may increase or decrease the contact angle of the evaporating sessile drops, depending on the evaporation rate. The thermocapillary convection in the drop induced by the evaporation enhances the effects of evaporation to suppress the spreading.

INTRODUCTION

The spreading of an evaporating liquid on a solid surface occurs in many practical processes, including thermal engineering. The typical processes concerned with heat transfer are film cooling, heat transfer in boiling and heat pipes.

Spreading of nonvolatile liquid droplets on a horizontal solid surface is a simple and useful tool in the study of the free-boundary problem, and therefore has been well studied by many investigators. A comprehensive review was made by Leger and Joanny [1]. The lack of volatility of the liquid implies the conservation of mass and volume, and thus simplifies the theoretical analysis. However, the occurrence of evaporation of common liquids is inevitable in practical processes. A well understanding of the evaporation influences on the contact angle of the droplet in controlled environment conditions is important in the study of the spreading. Recently, Anderson and Davis [2] analytically studied spreading of a two-dimensional volatile liquid droplet on a uniformly heated horizontal surface using lubrication theory. Hocking [3] considered that the macroscopic contact angles deviates from the microscopic angle in slip region and found that the contact angle is increased by evaporation. Moosman and Homsy [4] also reported an increase in the apparent contact angle when evaporation is present. However, Shanahan and Bourgès [5, 6] concluded that evaporation from the liquid drop meniscus will lower the contact angle. Anderson and Davis also found the effects of Marangoni flow induced by the local surface tension gradient near the contact line on the spreading through their analysis. However, the Marangoni flow direction found in their study is directly opposite from that observed in Cazabat et al. [7] and Redon et al. [8]. Obviously, these contradictions indicate that the dominant mechanism of the spreading of the evaporating drop is not clear yet. Further experimental studies using appropriate techniques are needed.

The most common method to measure the contact angle, the contact radius, and the height of a sessile drop on a solid surface is to view the drop from its edge through an optical microscope. This method can give only local information in the view direction. Zhang and Yang [9, 10] developed a laser shadowgraphy method to investigate the evaporation of sessile drop on a glass plate. The whole periphery of the drop can be tested simultaneously and the instantaneous drop size, including the contact diameter, the maximum height of the drop, and volume-time history can be determined. Allain et al. [11] used the same method to measure the contact angle of sessile drops. Due to the fuzzy outer rim of the projected shadow of the drop for the diameter of the drop is only an order of 1 mm, a considerable large error resulted in the measurement. This problem becomes more serious for a volatile liquid sessile drop when its base diameter contracts rapidly during the evaporation. Based on the laser shadowgraphy method developed by Zhang and Yang, we suggested a new optical arrangement to measure the contact angle and the evaporation rate of a sessile drop with much higher accuracy [12, 13].

The present study focuses attention on the effects of evaporation/condensation and thermocapillary convection on the spreading process and the evolution of the contact angle.

EXPERIMENTAL METHOD

A hybrid optical system of laser shadowgraphy and direct photography developed by Zhang and Chao [12, 13] was used in the present study. The hybrid optical system is briefly schematically shown in Fig. 1. A laser beam and a white light beam were collimated to horizontally parallel beams and then reflected by a splitter to perpendicularly pass through a test section without obstructing to view the tested drop from top. The test section was made of a microscope glass slide as the bottom and four pieces of plastic plate as the side walls. Two liquid reservoirs were put in the test section. For the experiment of the drop spreading in the saturated vapor environment, using another 1 mm thick rectangular microscope glass slide to cover the test section, sealed with Dow Corning high vacuum grease to form a hermetic box. The two glass slides were adjusted to parallel each other enabling the parallel lights passing through the drop vertically and the drop being viewed from top without distortion. In order to create a nonsaturated vapor environment three pieces of 1 mm thick microscope glass slides were used to constitute the cover. One was used as the main cover and fixed at the middle of the test section with the vacuum grease, which was adjusted to parallel with the bottom of the test section. Others were placed at the both sides of the main cover and can be slid laterally to function as a shutter to control the opening of the cover. It should be noted that the evaporation/condensation rate of the sessile drop varies with the vapor environment and dramatically affects the spreading characteristics of the drop. Therefore, we measured the evaporation/condensation rate through the volume-time history of the tested drop rather than the saturation level.

The laser beam was used to produce a refractive image of the sessile drop on a screen and white beam was used to get shaper photograph of the top view of the drop. The refractive image on the screen was recorded by a video recording system (system I), which constituted by a CCD camera with a video recorder and a monitor. Meanwhile, another video recording system (system II) was used to record the top view of the sessile drop. Both the recording systems can replay frame-by-frame with 30 frames per second.

Before each test the bottom glass slide of the test section was cleaned by ethanol and wiped by Olympus lens cleaning tissues, and then was shelved in open air, covered by a soft tissue, at least 24 hours. The bottom slide surface then became free of residual liquid molecules while remaining intact from impurity of the ambient air. The tested liquid was carefully deposited on the bottom surface by a micro-syringe to form a 1.5 to 4 μl sessile drop. The origin of the spreading and evaporation time, t, was taken at the moment when the micro syringe was detached from the liquid body.

The evolution of contact diameter, $d(t)$, is directly measured by the top view recorded by the recording system I. The tested drops are relatively small and are not deformed significantly by gravitational effects and therefore, can be considered to be sphere caps functioning as a plano-convex lens with a good approximation. The method developed by Zhang and Yang [9] is used to determine the evolution of the contact angle, $\theta(t)$, and the volume of the drop, $V(t)$. By a vary simple geometric relationship, the following expressions were derived:

$$\theta(t) = Arc\sin\frac{d(t)}{2\cdot R(t)} \tag{1}$$

$$V(t) = \pi\cdot h^2(t)\cdot[R(t) - \frac{h(t)}{3}] \tag{2}$$

Here, $h(t)$ is the maximum instant height of the sphere cap which is determined by

$$h(t) = R(t) - \sqrt{R^2(t) - d^2(t)/4} \tag{3}$$

where $R(t)$ is the instant curvature radius of the liquid sphere cap, which can be calculated from $R(t) = (n-1)\cdot s\cdot d(t)/[D(t)+d(t)]$, where n is the refractive

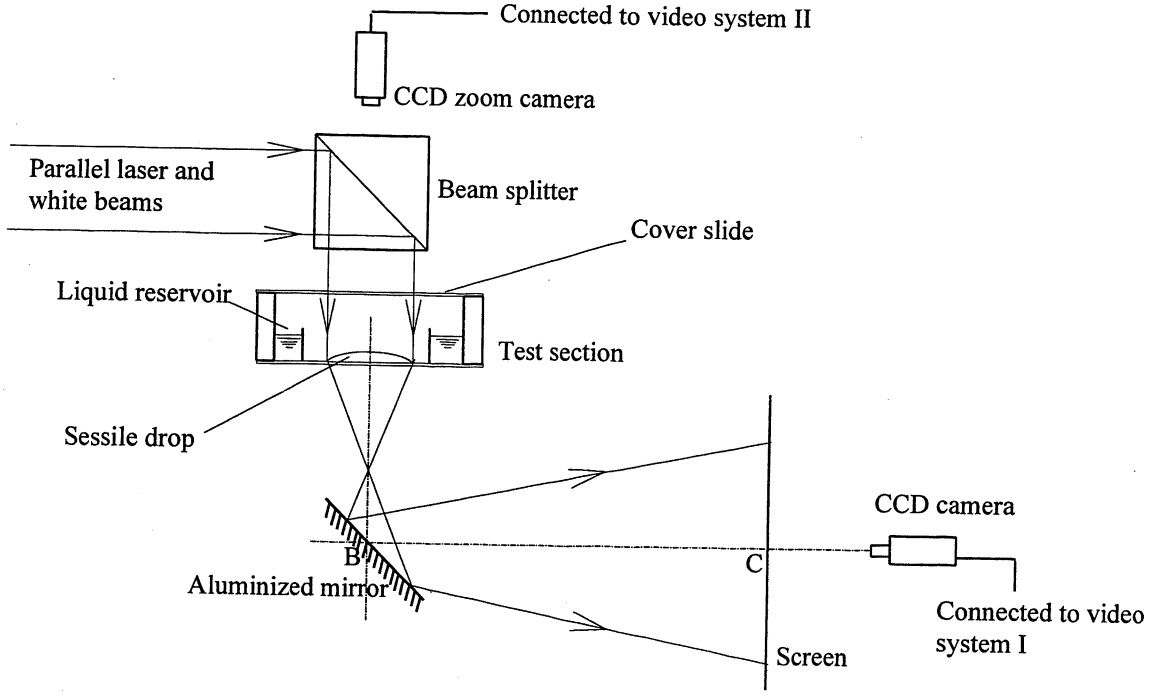

Fig. 1 Hybrid optical arrangement for measurements of spreading and contact angle

index of the liquid, s is the drop-screen distance from the center considered as an important parameter to measure the evaporation strength which can be determined by

$$\overline{w} = \frac{V_o}{t_f} \tag{4}$$

where V_o is the initial volume of the sessile drop (the drop volume at $t=0$), t_f is the lifetime of the tested drop. The instant evaporation rate, $W(t)$, can be calculated by $W(t)=\Delta V(t)/\Delta t$, where $\Delta V(t)$ is the difference of volumes between the measuring time interval Δt.

Figure 2 shows a typical picture of the drop top view and its correspondent refractive image on the screen with the drop-screen distance, s, of 630.0 mm. The pictures were taken at the moment of 1.97 sec. after an R-113 drop of 4 μl was placed on the bottom surface of the test section in open air at the room temperature 24 °C and the relative humidity of 44%. It can be seen that, from Fig. 2(a), $d(1.97)$=5.23 mm, and from Fig.2(b), $D(1.97)$=93.33 mm. Then, the instant contact angle, the maximum instant height of the drop, and the instant volume of the drop can be calculated from Eqs. (1) to (3): $\theta(1.97)$=12.704°, $h(1.97)$=0.291 mm, $V(1.97)$=3.140 mm^3.

RESULTS AND DISCUSSION

Three typical volatile liquids, freon-113 (R-113), cyclohexane, and n-pentane, were tested in different environments. The initial volume of the sessile drops was controlled less than 4 μl and therefore the drop profiles can be taken as sphere caps. Experimental results show that evaporation/condensation and Marangoni convection induced by the evaporation strongly affect the spreading. Condensation promotes the spreading, but evaporation suppresses the spreading and tends to advance a contraction of the drop. The competition between the spreading power and a weaker evaporation results in a complex spreading process with a change of the evolution trend of contact angle and contact diameter. Strong evaporation can hold back the spreading and pushes the drop to monotonically contract. Although the average evaporation rates between the tested liquids differ by one order of magnitude, all of them show that a capillary spreading process dominates in the initial stage and is gradually overtaken by the effects of evaporation.

Effects of Evaporation/condensation:

When an R-113 drop of 2.45 μl is placed on the glass surface in the saturated vapor environment at room temperature 24 °C, it rapidly spreads over on the surface. Due to the tendency of complete wetting, the contact diameter of the drop continuously increases and the drop finally becomes a thin film. The thickness of the wetting film results from a competition between long-range forces and spreading power, which is defined as

$$S = \gamma_{sv} - \gamma_{sl} - \gamma_{lv} \tag{5}$$

where γ_{sv} is the surface energy of interface between the solid and the vapor, γ_{sl} and γ_{lv} are the interface tension between the solid and the liquid, and the interface tension between the liquid and the vapor, respectively. As pointed out by Brochard-Wyart et al. [14], the long-range van der Waals forces tends to thicken the film, and the spreading power favors a large wet region. The major spreading process takes place within 1.5 seconds. Figure 3 (a) shows the evolution of the contact diameter, the contact angle, and the volume of the drop. Both the contact diameter and the volume of the drop monotonously increase while the contact angle decreases. The condensation at the contact line region plays a crucial role to renormalize the effective value of the spreading power making the drop completely wetting. The solid surface placed in the saturated vapor environment is certainly moistened, and therefore the physical chemistry properties of the surface are changed, especially the surface energy of the solid surface. It serves the mechanism of the variety of wetting characteristics.

The most complex and interesting case of this study is the drop spreading under a nonsaturated vapor environment. We tested a drop of 1.75 μl under the nonsaturated vapor environment at room temperature 24 °C, with an average evaporation rate of 0.032 μl/sec. The evolution of the contact

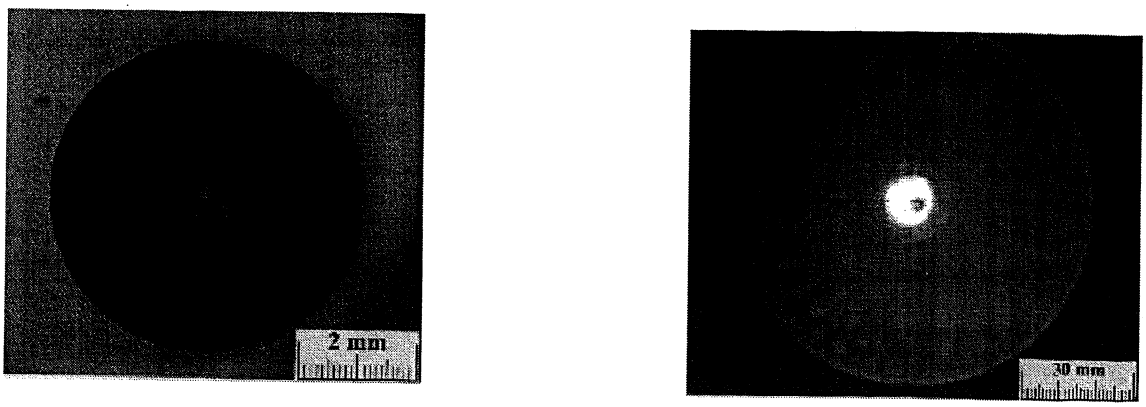

(a) Direct top view

(b) Refractive image

Fig. 2 Typical picture of the top view of a sessile drop and its refractive image

diameter, the contact angle, and the drop volume is shown in Fig.3 (b). The whole process can be divided to three stages: 1) The drop rapidly spreads out on the surface first, promoted by condensation of the vapor. It is referred as condensation-spreading stage. In this stage, both the contact diameter and the drop volume increase while the contact angle decreases sharply. 2) When the evaporation dominants the mass transfer between the drop and the vapor environment, both the contact diameter and the drop volume decrease while the contact angle increases, referred as evaporation-retracting stage. In this stage, the competition between evaporation effects and the spreading power turns the spreading of the drop onto a continuous retraction. In the mean time, the contact angle remains at a constant value for a while and then successively increases. 3) When the drop contact diameter retracts to a certain value (here it is 2 mm), the contact angle turns to decrease and the drop contracts more and more rapidly till drying up, referred as rapid contracting stage. In this last stage, the decrease of both the contact diameter and the contact angle is gradually accelerated, though the evaporation rate is slowing down, due to the restrain of geometry relation.

Effects of Evaporation Rate:

In order to test the effects of evaporation rate on the drop spreading and the evolution of the contact angle, three volatile liquids, cyclohexane, n-pentane, and R-113, were tested in open-air environment at room temperature (23 °C) and relative humidity of 44%. Generally, four stages have been observed: (1) initial spreading; (2) spreading-evaporation competitive balance; (3) evaporation dominating contraction; and (4) final rapid contraction. The higher the evaporation rate is, the shorter the initial spreading exists. Typical cases are described as follows. A cyclohexane sessile drop of initial volume 1.91 μl has a lifetime 56.83 seconds with the average evaporation rate of 0.034 μl/sec. The drop rapidly spreads initially, expanding its contact diameter from 3.81mm to 5.01 mm within 3 seconds, and then maintains its contact diameter unchanged for about 1.5 seconds in which the effects of evaporation and spreading reach a competition balance. After evaporation dominates the evolution process the drop almost linearly contracts to about 2 mm in contact diameter and then rapidly contracts till vanishing, as shown in Fig. 4 (a). Correspondingly, an n-pentane sessile drop has much higher evaporation rate and so shorter spreading period. For example, an n-pentane drop of initial volume of 1.61 μl has a lifetime 7.2 seconds with the average evaporation rate of 0.22 μl/sec. The n-pentane drop has the same evolution behavior of the contact diameter as the cyclohexane drop, but spreads only 0.4 seconds, as shown in Fig. 4 (b). It is noted that the final rapid contraction stage also starts at the contact diameter of about 2 mm.

The evolution of contact angle of a sessile drop for different liquids is quite different. For drops with lower evaporation rates, the contact angle decreases in the initial spreading and the spreading-evaporation balance stages. It increases linearly in the evaporation-dominant contraction stage and then rapidly grows in the final rapid-contraction stage, as shown in Fig. 4 (a). Obviously, evaporation increases the contact angle because of a large evaporative loss near the drop edge. For the drops with higher evaporation rates, the contact angle decreases monotonically and has a contact-angle plateau in the evaporation-dominant contraction stage. Although the evaporation generally would increase the contact angle, at the point where the stronger evaporation consumes the liquid volume of the drop large enough the contact angle turns to decrease. The characteristics of the evolution of the contact diameter and the contact angle are shown in Fig. 4 (b) and (c).

It is of interest to note that although the evaporation rate of R-113 sessile drops is lower than that of n-pentane sessile drops, the initial spreading stage of an R-113 drop is much shorter than that of an n-pentane drop. For example, an R-113 sessile drop with an initial volume of 2.36 μl has a lifetime of 19.2 second, but the period of initial spreading stage has only 0.2 seconds, as shown in Fig. 4 (c). It is also noted that the spreading-evaporation balance stage is too short to detect. This implies that there is another physical process that affects the evolution of the contact diameter.

Effects of Thermocapillary Convection

Thermocapillary convection in sessile drops can be induced by evaporation only under certain conditions, depending on the properties of the volatile liquids. Of the three liquids tested in this study, the cyclohexane drops, with initial volumes of 1.5 μl to 5 μl, exhibit no convection throughout their lifetime. The convection in n-pentane drops occurs near the end of the second stage (the spreading-evaporation balance stage). For example, for the n-pentane drop with an initial volume of 1.61 μl, convection appears at about 1 second after the drop begins to spread. Before then there is no convection in the drop at all. However, the thermocapillary convection in the R-113 sessile drops is induced by evaporation from the very beginning, even before the syringe detaches from the drops. The typical image of the convection in the R-113 drops is shown in Fig. 2 (b).

Due to the strong thermocapillary convection in the R-113 sessile drops, the evolution of the contact diameter is different from that of both cyclohexane and n-pentane drops. The thermocapillary convection in sessile drops obviously prevents the drops from spreading, enhancing the evaporation effects to suppress the spreading in the evolution of contact diameter. That is why the R-113 drop has very short initial spreading stage comparing to n-pentane drop and an undetectable spreading-evaporation balance stage, though its evaporation rate is much lower than one of n-pentane. It is interesting to note that the R-113 drop accelerates contraction after its contact diameter reaches 2 mm, too.

Uncertainty analysis

The method of single sample experiments was utilized to estimate the uncertainties in both θ and V through Eqs. (1) and (2). The maximum uncertainty occurs in the end of the final stage for R-113 sessile drop evaporating in open air, in which d=0.82±0.019mm and D=76.2±0.22mm. The uncertainty for the contact angle is 2.78% and for the drop volume is 10.68%, respectively.

CONCLUSIONS

Experimental results of evaporating sessile drops on a glass-slide surface for three volatile liquids show that the evaporation/condensation and thermocapillary convection strongly affect the drop spreading and contact angle. The main conclusions are summarized as follows:

1. Evaporation/condensation plays a crucial role in the wetting and spreading of volatile liquid drops and greatly affects the evolution of the contact angle and the contact

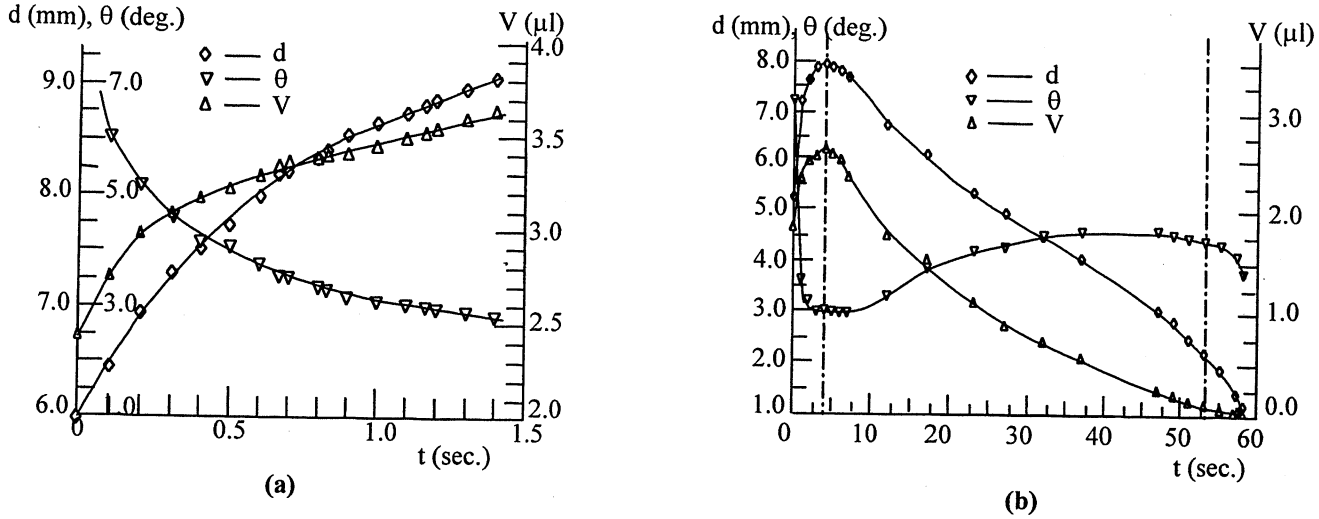

Fig. 3 Evolution of contact diameter, contact angle, and volume of an R-113 sessile drop: (a) in saturated vapor environment with initial volume of 2.45 μl, (b) in a nonsaturated vapor environment with initial volume of 1.75 μl.

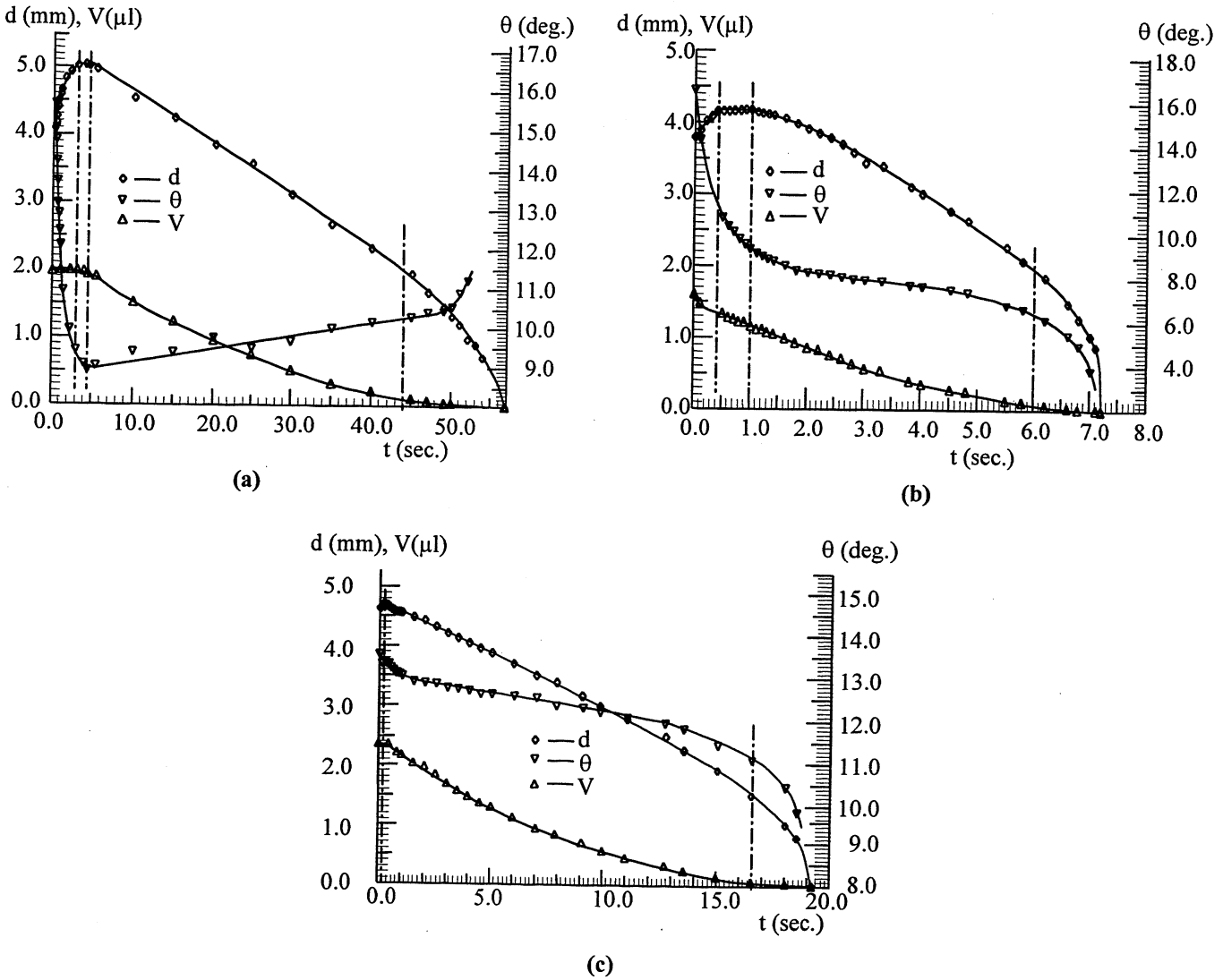

Fig. 4 Evolution of contact diameter, contact angle, and volume of a sessile drop in open air: (a) cyclohexane drop, (b) n-pentane drop, (c) R-113 drop

diameter of the drop. An R-113 drop placed in three different vapor environments presents quite different spreading characteristics. Condensation promotes the spreading, but evaporation suppresses the spreading and favors contraction of the drop. The competition between a weaker evaporation effects and the spreading power results in a complex spreading process turning the drop spreading onto a continuous retraction. Strong evaporation can hold back the spreading and pushes the drop to monotonically contract. When the contact diameter of an evaporating sessile liquid drop decreases to a certain value, the contraction of the drop is gradually accelerated till trying up, though the evaporation rate of the drop is slowing down.

2. An evolution of contact diameter of a sessile drop evaporating in open air can be divided into four stages: 1) initial spreading; 2) spreading-evaporation balance; 3) evaporation-dominant contraction; and 4) rapid contraction. Drop spreading always exists at the early initial spreading stage in the evolution of contact diameter of an evaporating liquid sessile drop, even if the drop has a considerably high evaporation rate, but is rapidly taken over by the effects of evaporation.
3. Thermocapillary convection induced by the evaporation enhances the evaporation effects on the evolution of the drop contact diameter and the contact angle to surpass the spreading and shortens the spreading-evaporation balance stage to become undetectable.
4. The contact angle of sessile drops with low evaporation rate is increased by evaporation. However, strong evaporation decreases the contact angle to create a contact-angle plateau in the evaporation-dominant contraction stage.
5. The evaporation of sessile drops always accelerates contraction when their contact diameter reaches 2 mm.

REFERENCES

1. L. Leger and J. F. Joanny, Liquid spreading, *Rep. Prog. Phys.*, pp. 431-486, 1992.
2. D. M. Anderson and S. H. Davis, The spreading of volatile liquid droplets on heated surfaces, *Phys. Fluids,* vol. 7, pp. 248-265, 1995.
3. L. M. Hocking, On contact angle in evaporating liquids, *Phys. Fluids,* vol. 7, pp. 2950-2955, 1995.
4. S. Moosman and G. M. Homsy, Evaporating menisci of wetting fluids, *J. Colloid Interface Sci.,* vol. 73, pp. 212-223, 1980.
5. M. E. R. Shanahan and C. Bourgès, Effects of evaporation on contact angles on polymer surfaces, *Int. J. Adhesion and Adhesives,* vol. 14, pp. 201-205, 1994.
6. C. Bourgès-Monnier and M. E. R. Shanahan, Influence of evaporation on contact angle, *Langmuir,* vol. 11, pp. 2820-2829, 1995.
7. A. M. Cazabat, F. Heslot, S. M. Troian, and P. Carles, Fingering instability of thin spreading films driven by temperature gradients, *Nature,* vol. 346, pp. 824-826, 1990.
8. C. Redon, F. Brochard-Wyart, and F. Rondelez, Festoon instabilities of slightly volatile liquids during spreading, *J. Phys. II (France),* vol. 2, pp. 1671-1676, 1992.
9. N. Zhang and W. J. Yang, Natural convection in evaporating minute drops, *J. Heat Transfer,* vol. 104, pp. 656-662, 1982.
10. N. Zhang and W. J. Yang, Visualization of evaporative convection in minute drops by laser shadowgraphy, *Rev. Sci. Instrum.,* vol. 54, pp. 93-96, 1983.
11. C. Allain, D. Ausserre, and F. Rondelez, A new method for contact-angle measurements of sessile drops, *J. Colloid Interface Sci.,* vol. 107, pp. 5-13, 1985.
12. N. Zhang and D. F. Chao, A new approach to measure contact angle and evaporation rate with flow visualization in a sessile drop, *International Conference on Interface Problems,* Aug. 16-18, 1999, Monterey, California, U.S.A. *and NASA/TM-1999-209636,* 1999.
13. N. Zhang, and D. F. Chao, Effects of Evaporation/Condensation on Spreading and Contact Angle of a Volatile Liquid Drop, *Heat Transfer Science and Technology 2000,* Higher Education Press, Beijing, pp. 367-372, 2000.
14. F. Brochard-Wyart, J. M. di Meglio, D. Quere, and P. G. Gennes, Spreading of nonvolatile liquids in a continuum picture, *Langmuir,* vol. 7, pp. 335-338, 1991.